In Vivo Diffusion Tensor Imaging of Human Optic Nerve Using 2D Interleaved Inner Volume Technique on 3T System

S-E. Kim[1], E-K. Jeong[1], T. H. Kim[1], J. R. Hadley[1], E. Minagla[1], J. Anderson[1], and D. L. Parker[1]

[1]Utah Center for Advanced Imaging Research, Department of Radiology, University of Utah, Salt Lake City, Utah, United States

INTRODUCTION: Diffusion Tensor Imaging (DTI) of human optic nerve in vivo using 2Dsingleshot EPI is generally very challenging because of its small size and the presence of magnetic susceptibility artifacts. Although techniques other than 2D ss-EPI have been used for DTI of the human optic nerve [1,2], these techniques typically employ relatively thick slices and require a long scan time to overcome their intrinsic low SNR. Recent publications show that interleaved multiple inner volume (IMIV) imaging[3] or reduced field of View (rFOV) techniques[4,5] combined with EPI can reduce the geometric distortion and improve the accuracy of DTI measurements. In this work we present the DTI measurement of the normal human optic nerve using 2D IMIV DWEPI and 2D rFOV DWEPI. Each technique has a different inner volume realization using a pair of slice selective refocusing RF pulses with the selection gradient in the phase-encoding direction.

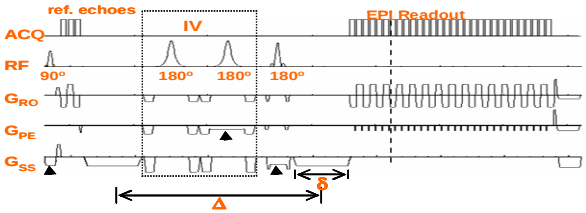

Figure 1. *2D IMIV DWEPI pulse sequence diagram.*

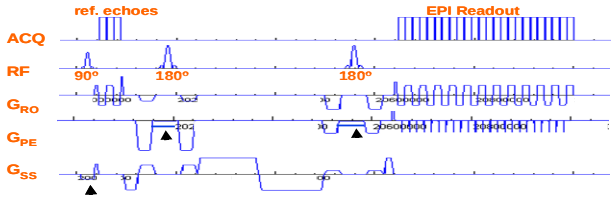

Figure 2. *2D rFOV TRSE DWEPI pulse sequence*

METHODS: A 2D ss-EPI pulse sequence was modified to implement 2D IMIV (Fig. 1) and rFOV (Fig. 2) DWEPI. As shown in Fig. 1, a pair of refocusing and inversion (RI) 180° RF pulses immediately follows the excitation 90° pulse to confine the reduced phase FOV for interleaved multiple slice imaging. These two RI pulses are separated by large spacing in 2D rFOV DWEPI as shown in Fig. 2. The rFOV was accomplished by applying the slice selective gradients for two RI pulses in the phase encoding direction. All MRI studies were performed using a 20 channel dedicated optic nerve coil[6] on a Siemens Trio 3T MRI scanner (Siemens Medical Solutions, Erlangen, Germany). The optic nerve DWI from three healthy volunteers were acquired using 2D IMIV-DWEPI and 2D rFOV DWEPI with the following parameters: FOV=160x52mm, matrix=160x52, TR=3s, TE=76 ms (IMIV) or 82 ms(rFOV), 12 magnitude averages, and interleaved acquisition of 8 contiguous slices. Diffusion gradients were applied along 12 directions using b-value of 0 and 500 s/mm^2. Total imaging time was 7:30 min (450s) for each method. DW images were post-processed using DTI analysis software written in IDL (Research Systems Inc., Boulder, CO) to calculate ADC maps, the six independent diffusion tensor components, the eigenvalues and eigenvectors, fractional anisotropy (FA), and to visualize the results using a RGB representation of the principal eigenvector. The two regions-of–interests (ROIs) including only the center of the left and right optic nerve were manually selected on b_0 images and then transferred to calculated FA maps to measure the fractional anisotropy, the principal eigenvalue ($\lambda_{\|}$) and the mean of the other two orthogonal eigenvalues ($\lambda_{\perp}$). Here, $\lambda_{\|}$ and $\lambda_{\perp}$ indicate the diffusivities in the axial and radial directions of the fiber with cylindrical symmetry.

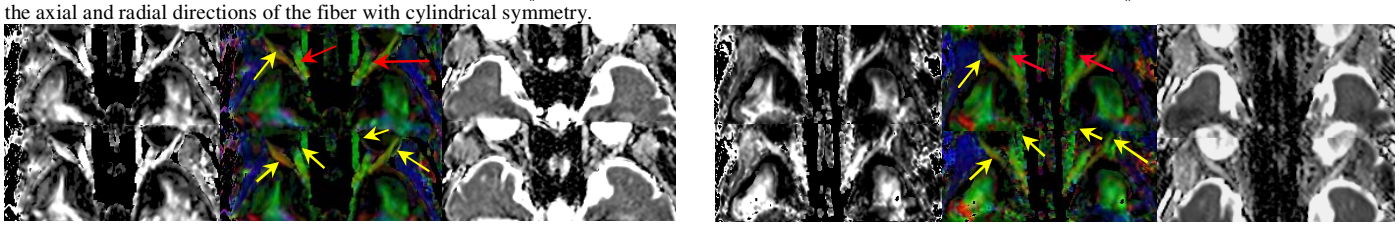

Figure 3*. DTI measurements of a healthy human optic nerve using 2D IMIV(a) and rFOV(b) EPI: fractional anisotropy (1st column), principal eigenvector maps (2nd column), ADC map (3rd column). The color coding: red - L/R, blue – S/I, green A/P.*

RESULTS & DISCUSSIONS: The mean values of FA, $\lambda_{\|}$, $\lambda_{\perp}$, and diffusivity were calculated across subject on the central slice of the optic nerve. The values using the two pulse sequences are similar to each other. The mean diffusivity and FA values shown in table 1 are close to values reported previously using other DTI acquisition methods[1,2,5].Although our measured values of $\lambda_{\|}$ and $\lambda_{\perp}$ were relatively lower than the values (2.0×10^{-3}mm^2/s and 0.84×10^{-3}mm^2/s) reported in other studies[2], the ratio ($\lambda_{\|}/\lambda_{\perp}$) is almost similar to the value (2.3 or 2.04) previously reported[2,5]. It may be necessary to increase the b-value to increase the accuracy of measurement of $\lambda_{\|}$ and $\lambda_{\perp}$. Fig. 3 illustrates FA, principal eigenvector, and ADC maps using 2D IMIV DWEPI (a) and 2D rFOV DWEPI (b) from the same volunteer. The FA and ADC maps demonstrate the detailed structure of the optic nerve and less distortion comparing to DTI using a routine 2D ss-EPI. Although a short ETL (52 in the current study) was used, some distortions caused by $\mathbf{B}_o$ field inhomogeneity due to susceptibility variations between soft tissues and air (sinus) are evident. The principal eigenvector maps using 2D IMIV DWEPI demonstrate more clear fiber coherence of the area around the optic nerve(red arrow) and ocular muscle(yellow arrow). This result indicates that both 2D IMIV DWEPI and 2D rFOV DWEPI allow reliable DTI measurement of optic nerve and ocular muscle. Quantitative analysis of diffusivity and anisotropy in the human optic nerve and ocular muscle appears to be feasible and has potential to enable more sensitive and specific detection and monitoring of structural changes caused by pathology including multiple sclerosis, optic neuritis, and neurofibromatosis.

	FA	Mean Diffusivity ($\times10^{-3}$ mm^2/s)	$\lambda_{\|}$ ($\times10^{-3}$ mm^2/s)	$\lambda_{\perp}$ ($\times10^{-3}$ mm^2/s)	Ratio($\lambda_{\|}/\lambda_{\perp}$)
IMIV	0.456±0.021	1.17±0.23	0.85±0.11	0.36±0.079	2.36±0.23
rFOV	0.499±0.050	1.02±0.15	0.85±0.15	0.38±0.061	2.20±0.07

Table 1 *DTI values measured from normal human optic nerve.*

ACNOWLEDGEMENT: ***Supported by NIH grants R01 HL 48223, HL 57990 and EY015181, Cumming Foundation, Margolis Foundation, and Siemens Medical Solutions.***

REFERENCES: 1. Bastin ME, *MRM*.2002;**48**:6. 2. Wheeler-Kingshott CAM, et al. *MRM*.2006;**56**:446. 3. Jeong EK, et al. *MRM*.2005;**54**:1575. 4. Jeong EK, et al. *MRM*. 2006;**56**:1173. 5. Xu JG, et al. *ISMRM*. 2007;**15**:11. 6. Hadley JR, et al. *ISMRM* 2007;**15**:1055.